EUROFUSION WPJET1-PR(16) 14727

GF Matthews et al.

Energy Balance in JET

Preprint of Paper to be submitted for publication in
22nd International Conference on Plasma Surface Interactions
in Controlled Fusion Devices (22nd PSI)

This work has been carried out within the framework of the EUROfusion Consortium and has received funding from the Euratom research and training programme 2014-2018 under grant agreement No 633053. The views and opinions expressed herein do not necessarily reflect those of the European Commission.

Energy Balance in JET

G.F.Matthews[a*], P.Bunting[a], S.Devaux[b], P.Drewelow[c], C.Guillemaut[d], D.B.King[a], E.Lerche[e], S.Silburn[a], G.Szepesi[a], V.Riccardo[a], V.Thompson[a] and JET Contributors[f]

EUROfusion Consortium, JET, Culham Science Centre, Abingdon, OX14 3DB, UK
[a]CCFE, Culham Science Centre, Abingdon, OX14 3DB, UK
[b] IJL, UMR 7198 CNRS, Universite de Lorraine, 54500 Vandoeuvre les Nancy, France
[c] Max-Planck Institute für Plasma Physik, Euratom Association, 17491 Greifswlad, Germany
[d] IST, IPFN - Laboratório Associado, IST, Lisboa, Portugal
[e]LPP-ERM/KMS, Association EUROFUSION-Belgian State, TEC partner, Brussels, Belgium
[f]Appendix of F. Romanelli et al., Proc. of the 25th IAEA FEC 2014, Saint Petersburg, Russia
Corresponding/presenting author e-mail: gfm@jet.uk

Corresponding/presenting author address[a]

PSI-22 Keywords: ILW, JET

PACS: 52.40.Hf, 52.55.Fa, 52.55.Rk

Abstract

In this paper we discuss results from the study of the energy balance in JET based on calculated heating energies, radiated energy from bolometry and tile calorimetry. Recent data enables us to be more confident in the numbers used and to exclude certain possibilities but the overall energy imbalance which typically amounts to 25% of total input remains unexplained. This shows that caution is required in interpreting fractional radiated powers which are commonly used to measure the effectiveness of impurity seeded scenarios at reducing divertor heat load.

1. Introduction

The total energy input into a tokamak during the pulse must equal that lost to the plasma facing components (PFCs). Quantifying this balance is essential for knowing what radiated power fraction you have and what the PFC power/energy loadings really are – particularly in the main chamber. For reactor scale devices such as ITER or DEMO, even a small fraction of the combined external plus alpha particle heating power could cause serious damage if not distributed over a large enough area of the first wall. The plasma heating systems used in current devices are also complex and so there is a potential for error in evaluating the input power and such errors could have implications for many different aspects of tokamak physics such as plasma transport and calculation of fusion neutron production rates.

The energy losses to the PFCs can be difficult to determine accurately. Although infra-red diagnostics work well when studying the hottest areas of the vessel, there are many complications such as reflections, uncertain surface emissivity and non-thermal IR emission from the plasma which put accurate power accounting (at the level we require) beyond reach in current devices such as JET. The alternative approach, which we discuss here, is the use of thermocouple (TC) based tile calorimetry and bolometers. The divertor and main chamber tiles used in JET's ITER-like Wall [1] are inertially cooled and due to the engineering need to allow unhindered thermal expansion, the thermal contact with support structures is generally poor. This means long cooling times compared to the time it takes a tile to reach internal thermal equilibrium. As a result, JET tiles make good calorimeters [2], [3]. Recent efforts to validate the simple methods used in analysis of the thermocouples against the finite element thermal calculations using ABAQUS have revealed that the temperature dependence of the heat capacity of carbon fibre composite (CFC) has a significant effect on the results and was not correctly implemented previously [2]. This benchmark is described in section 2 along with the currently estimated inherent uncertainties due to approximations required for the analysis of real data. Given that JET has limited numbers of thermocouples in recessed areas, the energy arriving on the divertor and limiter tiles is only one part of the equation and in addition we need the radiated energy measured by bolometers and the inputs from the heating systems including the ohmic heating due to the plasma current, see equation (1):

$$E_{Ohm} + E_{NBI} + E_{ICH} = (E_{Pdiv} + E_{Rdiv}) + (E_{Plim} + E_{Rlim}) + (E_{Pwall} + E_{Rwall}) \qquad (1)$$

where E_{Ohm}, E_{nbi} and E_{ich} are the Ohmic heating, absorbed neutral beam injection power (NBI) and ion cyclotron heating (ICH) energy inputs respectively. The other side of the equation is comprised of the energy losses to the divertor, limiters and remote areas of the wall where subscript 'P' refers to plasma related load and 'R' the electromagnetic radiation and neutral losses. In terms of what we actually measure this can be rewritten as:

$$E_{Ohm} + E_{NBI} + E_{ICH} = E_{TCdiv} + E_{TClim} + (E_R - f_B E_{RB} – f_X E_{RX}) \qquad (2)$$

Where E_{TCdiv} and E_{TClim} are the divertor and wall total energies from thermocouples, $E_R=E_{RD}+E_{RB}$ is the total radiated power from JET's bolometers. The last two terms allow for the fractions (f_B, f_X) of the bulk plasma (main chamber) and X-point/divertor radiated energies (E_{RB}, E_{RX}) falling on the divertor and limiter tiles which are therefore double counted. An analysis which compares tomographic inversions with the standard JET intershot analysis of bulk and divertor radiation shows that $f_B \sim 0.11$, $f_X \sim 0.27$ (after correction for the fact that we are not using Tile 5 thermocouple data). These values are used as the default in section 3.

In deriving (2) we have also assumed that negligible plasma related energy is deposited on recessed areas of the wall ($E_{Pwall}=0$). Although there is evidence for strong radial plasma transport in the far SOL under detached conditions [4], the sparse thermocouple measurements in JET from recessed areas suggest that this does not extend much beyond the limiters and that overall the contribution is small. This is discussed further in section 4.

In section 3 we show that at high energy input we are typically missing ~25% of the energy input and in section 4 we discuss the local consistency of the wall energy contribution derived from bolometers. Finally, section 5 we discuss the possible causes for the energy imbalance and its implications.

2. Validation of the JET tile calorimetry method

The tile calorimetry method used at JET [2] is based on measuring the cool down of the tiles between pulses. This requires that the time taken for a tile to come into internal thermal equilibrium is short compared to the cooling time due to conduction and Planck radiation. When this is true we can back extrapolate the equilibrated temperature to the end of the JET pulse and use this to calculate an effective bulk temperature rise from which the increase in thermal energy can be calculated. The most critical tiles for the overall energy balance are the divertor tiles and the large temperature rises also mean that there are most likely to be errors due to the fact that the losses from the tile will not comply exactly with a simple exponential decay particularly when the temperature distribution, and hence sink terms, are non-uniform at the tile surfaces. Although with the ITER-like Wall Tiles 1,3,4,6,7,8 (Fig. 1) are CFC with a W-coating, this has minimal impact with respect to previous analysis with the carbon wall [2].

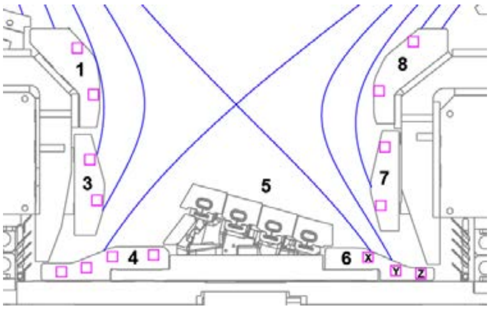

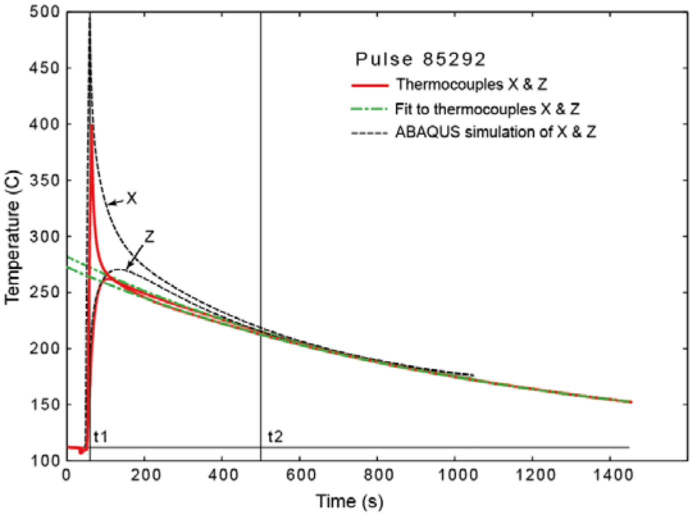

Fig. 1 Divertor TC locations and configuration for pulse 85292

Fig. 2 Tile 6 thermocouple data and equivalent ABAQUS simulations

To estimate the uncertainties, a specific divertor tile (Tile 6) has been fully modelled in 3D using the ABAQUS finite element code for a JET pulse with relatively high input energy (85292) [6]. This pulse had 16MW of NBI power applied for about 10s. The layout of thermocouples in the JET divertor and magnetic configuration for 85292 is shown in Fig. 1. The thermocouple data from two Tile 6 thermocouples are shown in Fig. 2 along with the ABAQUS simulations and exponential fits to the thermocouple data for times greater than 500s (t2) which are back extrapolated to the end of the pulse (t1). The fit parameters are the back extrapolated start temperature, the characteristic decay time and final equilibrium temperature.

Once the equivalent total temperature rise assuming internal equilibrium has been derived from back extrapolation of the thermocouple data, the total energy is calculated by integration of the temperature dependent heat capacity over the relevant temperature interval ($E_{tile} = m_{tile} \times \int C_p(T)dT$ where m_{tile} is the tile mass). The JET divertor is toroidally axisymmetric and so the total energy per row can be obtained simply by multiplying by the number of tiles in the toroidal set.

The match between ABAQUS and temperature histories during the pulse shown in Fig. 2 is not perfect because the power deposition profile was approximated in a simple way using a skewed triangular function. However, the cool down has been made a reasonable match to the experiment through adjustment of the thermal contact resistance between the W-coated CFC tile and the CFC baseplate within the ABAQUS model. Planck radiation is included but switching it on and off shows that it plays a relatively minor role. It is the cooling phase which is most important for our method.

2.1 Sources of error in the divertor tile calorimetry method

The best estimate of the energy delivered to Tile 6 in reference pulse 85292 derived using ABAQUS simulations is 38.6MJ. Six Tile 6 thermocouples are available for this pulse spread over 3 different toroidal locations. Back extrapolating the data from each thermocouple independently and multiplying by the 96 tiles in the toroidal set, gives energies in the range 34-42MJ depending on which thermocouple is used. If we average these data we get find 37.4MJ with a standard deviation of 3MJ. The incorrect integration of the temperature dependent heat capacity used in [2] would give a result of 50.7MJ.

The ABAQUS simulated temperatures are most useful for testing the sensitivity of the back extrapolation method to details of the heat deposition. Different temperature histories during the pulse were obtained by shifting strike point locations (-1 to 3cm shift from nominal), varying profile widths (30-120mm) and adjusting toroidal wetted fractions (70%-100%) while keeping the same input energy. This study used a fixed input of 35MJ and the fit for the 8 different cases produced energies ranging from 37.1-38.3MJ hence an overestimation of the energy by an average of 7%.

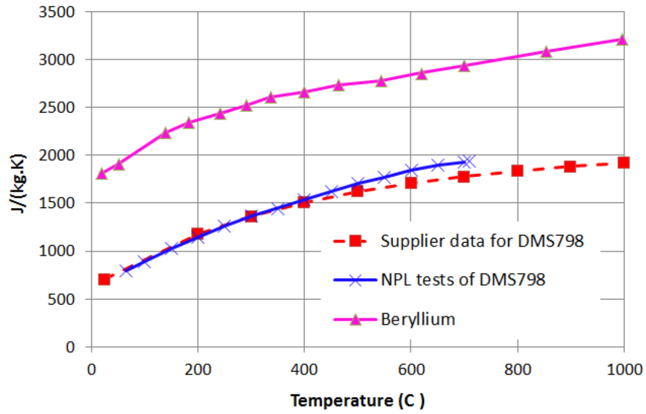

Fig. 3 Temperature dependent heat capacities for CFC type DMS798 used at JET from supplier data and recent measurement at the UK National Physical Laboratory (NPL). Data for beryllium is also shown.

Another potential source of error for the calorimetry method is the uncertainty in material properties. In particular, the mass of the tile due to density variations intrinsic to CFC material manufacture and the reliability of the heat capacity data when applied to the CFC material used in JET (material produced by Meggitt to DMS798). The density range for this material is 1.72-1.90gcm^{-3} and the tile mass used in the calculations presented here corresponds to an average density of 1.85gcm^{-3}.

To be sure that the temperature dependent heat capacity our material was correct, we cut samples from the CFC used in JET and sent them for testing at the National Physical Laboratory in the UK. The results are compared with the pre-existing data in Fig. 3.

In addition to the W-coated CFC divertor tiles, there are 48 bulk W tile modules each containing 8 stacks of 24 tungsten lamellas giving a total of 9216 lamellas each ~6mm wide in the toroidal direction, Tile 5 in Fig 1. This segmented design has been chosen to minimise the risk of cracking the brittle tungsten elements due to thermal stresses and other forces. There are thermocouples attached to the underside of some lamellas but these have not worked reliably and even when the data is good the lack of toroidal heat diffusion leads to variability between lamellas that mean the data cannot be trusted for energy balance calculations. For this reason, in this paper we only analyse JET pulses where the strike points have avoided this tile. We assume that the plasma radiation going to the area occupied by Tile 5 is correctly determined by the bolometer system.

We conclude from the ABAQUS work that the intrinsic systematic uncertainty in the divertor tile calorimetry method is <±10% with respect to the determination of total energy received by each toroidal set of instrumented divertor tiles. If anything, there are indications that the assumptions and methods tend towards a slight over-estimation of the true divertor energy. On the other hand, there are tiles just outside the divertor which are not instrumented and could receive some plasma energy flowing along the magnetic field as in the example of Fig.

4 where plasma energy could arrive to left of the point marked s=0 on tiles without thermocouples. We discuss this point further in section 4 and we conclude that based on the energy distribution tile to tile within the divertor, this is unlikely to more than a 10% effect on total divertor energy. We therefore believe that the maximum uncertainty in the total divertor energy is <20%.

2.1 Sources of error in the limiter/wall tile calorimetry method

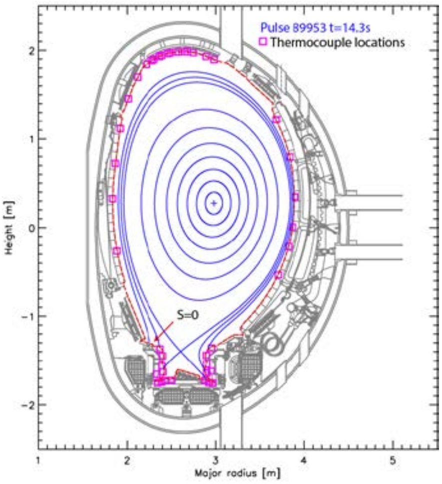

Fig. 4 Distribution of main chamber thermocouples and magnetic configuration for pulse 89953

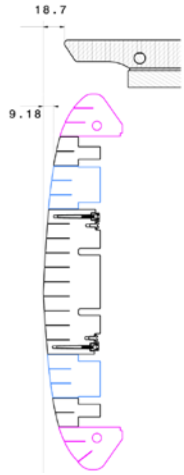

Fig. 5 Toroidal section through limiter 4B. There are 7 Be blocks and W-coated CFC re-ion protection tile (top). In all cases, only the middle blocks and their neighbours (blue) have thermocouples.

Beryllium, which is used for the majority of the instrumented limiter tiles, has less variable physical properties than the CFC over the relevant temperature range (JET limiter tiles usually start at temperatures above ~200ºC). The uncertainty in the energy calculated for each block is thought to be up to 10% due to limitations of the back extrapolation method.

The main issue for the accuracy of total energy accounting with the limiter thermocouples is the relatively sparse measurements radially and poloidally [3], Figs. 4&5, coupled with the limiter to limiter shadow pattern which due to the normal helicity in JET deposits more power on the right side of the limiters near the top and on the left hand side near the bottom [7]. In this paper, to estimate total energies we assume that each instrumented block is characteristic also of a number of its un-instrumented neighbours. We also multiply the calculated result by 1.6 to allow for the fact that the thermocouples only cover about one energy decay length (assumed to be ~1cm). This method has been benchmarked against limiter discharges and ~100% energy accounting is obtained, Fig. 6. However, this could be fortuitous since the estimated systematic error for the total limiter energy is ±30%. Although this level of uncertainty may sound large, the overall effect on the energy balance of diverted discharges is minimal because the total limiter energy is only ~5% of input. We therefore regard the limiter shots as way of calibrating the limiter energy calculation so that we can be sure it is giving reasonable values when applied to diverted discharges.

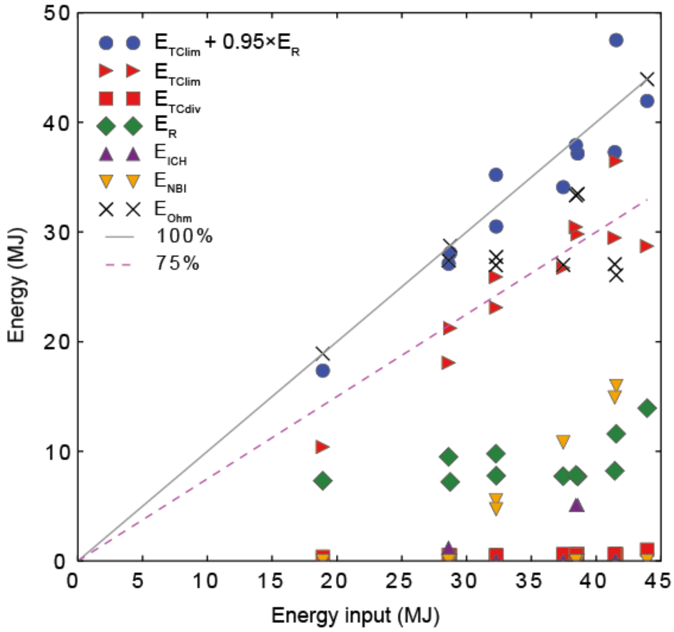

Fig. 6 Energy balance (circles) for limiter discharges on inner and outer limiters including Ohmic, ICRH and NBI heating. Also shown are individual energies which contribute.

Finally, there are some tiles in recessed areas between the limiters which were included to measure neutral beam shine-through on the inner wall and re-ionisation power on the outer limiters, Fig.5. Although few in number and not directly used in the energy balance calculations these have be used to validate the bolometer reconstructions in cases where the NBI related loads are small and show us that the plasma load in recessed areas is negligible, section 4.

3. Energy balance in diverted discharges

The energy balance according to equation (2) is plotted in Fig. 7 for a set of ~350 divertor discharges from JET ITER-like Wall in which the strike point was not on divertor Tile 5 throughout the pulse to get around its lack of thermocouple data. We can see from Fig. 7 that the scatter on the energy found is low but we are missing ~25% of the calculated energy input. We can also see that the energy balance improves at low input where ICRH and Ohmic heating are more important.

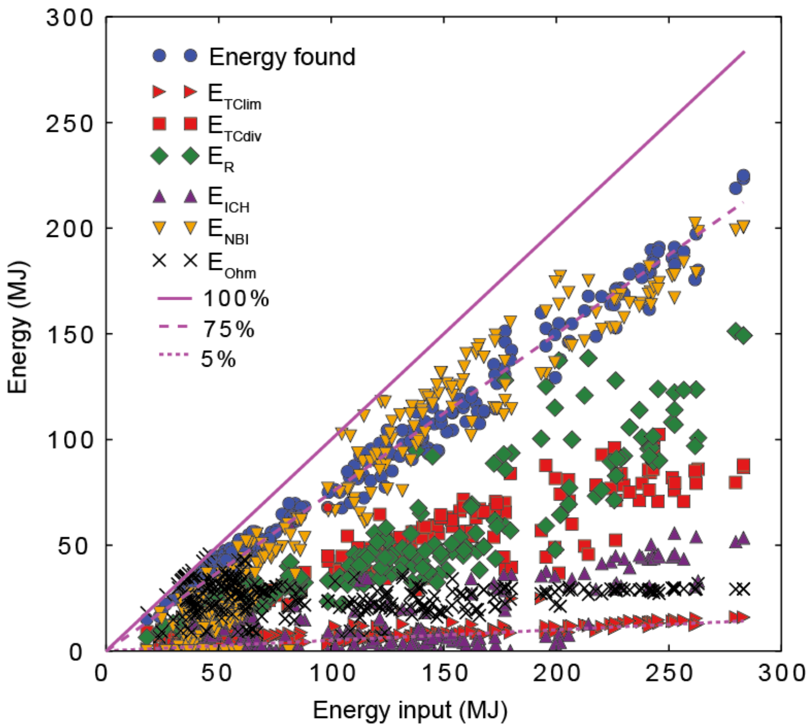

Fig.7 Energy balance (blue circles) for a set of ~350 divertor discharges including ohmic, ICRH and NBI energy. Also shown are the individual energies which contribute.

The idea that there might be systematic errors proportional to the different components of the energy balance has been explored by regression of the above data, Fig. 8, with expressions of the form given in Eqn. (3) (title row of Table 1). Up to 4 of the 5 parameters can be fitted at a time. Some of the variations which have been tried are given in Table 1. The residual chi-squared given in each case is normalised to the case where only parameters d and e are adjusted ($\chi^2 = 1$). The estimated errors on the fitted parameters are small in all cases quoted here (<4%) but the real issue is whether the model is correct.

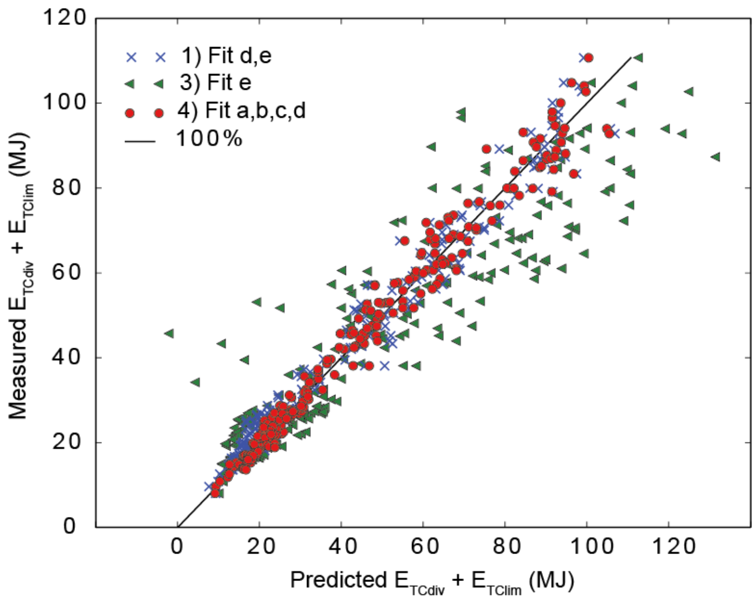

Fig. 8 Comparison of fit cases 1,3,4 from Table 1.

$a \times E_{oh} + b \times E_{nbi} + c \times E_{ich} = d \times (E_{TCdiv} + E_{Tclim}) + e \times (E_R$ - $f_B E_{RB} – f_X E_{RX})$ (3)							
Case	Parameters fitted	χ^2	a	b	c	d	e
1	d, e (reference)	**1**	**1**	**1**	**1**	1.68	1.04
2	a, b, c	1.05	0.80	0.65	0.97	**1**	**1**
3	e only	8.5	**1**	**1**	**1**	**1**	1.76
4	a, b, c, d / e=1.0	0.72	1.00	0.81	1.05	1.40	**1**
5	a, b, c, d / e=1.25	0.72	1.25	1.02	1.31	1.75	**1.25**

Table 1: Fit parameters defined in equation (3) and relative residual chi-squared for different combinations of pre-set factors (bold). Examples are plotted in Fig. 8. Factors f_B and f_X are introduced in section 1 and set to 0.11 and 0.27 respectively.

The only firm conclusion we can draw from these results is that if the missing energy is due to systematic errors which are constant across the data set, it is least likely that the source of the imbalance is due to the bolometer data alone. On the other hand, the χ^2 is rather similar whether the imbalance is assumed all due to the heating system inputs being overestimated (a,b,c) or due to a systematic under calculation of sink terms (d,e).

We cannot fit all the parameters in equation 3 without some constraint so we have chosen to fix factor e (radiation) to 1 in case 4. This minimises the overall χ^2 and still pushes the multipliers on NBI(b) and tile energy(d) outside of the range we are comfortable with but by less than before. Case 5 is exactly equivalent to case 4 but with a factor 1.25 applied to the radiation term which has the effect of increasing terms a,b,c and d by the same factor. To choose between these requires a view on the maximum plausible systematic error in each term and this is discussed further in section 5. However, we can see from case 5 that forcing the multiplier on the radiated power up to 1.25, allows the neutral beam input power to be correct but increases the multiplier needed on the thermocouple data to 1.75 (almost like having a second divertor somewhere). Overall it looks less credible than case 4.

4. Detailed comparison with bolometer tomography

Limiter thermocouples can be compared directly with tomographic reconstruction of the radiated energy pattern for a whole pulse. The bolometer reconstructions are based on averages of the raw data for each characteristic phase of the discharge so all data used but there is limited time resolution and no gaps in the data. An example which is important for what is presented here is shown in Fig. 9. Discharge 89953 is our chosen example because only the Octant 8 neutral beam injector (NBI) was used. This means that the recessed tiles designed to monitor Octant 4 re-ionisation and beam shine-though on the inner wall only see plasma radiation and any far SOL plasma. This discharge also started on the outer limiter and maintained a high clearance with much of the inner wall and top throughout the pulse.

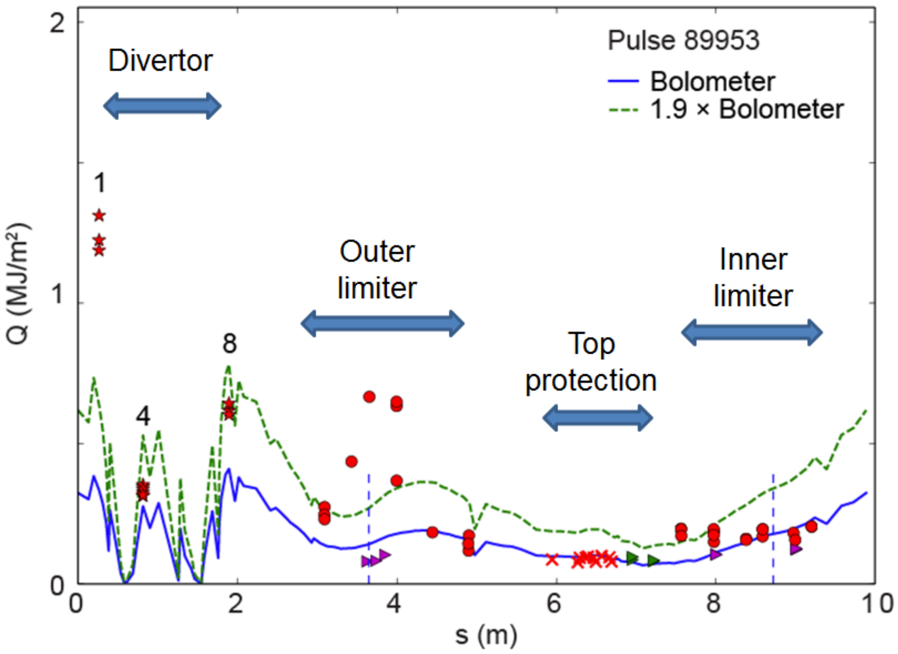

Fig. 9. Energy density derived from tile calorimetry(points), compared to tomographic reconstruction of bolometer data (solid line) for pulse 89953. The plasma maintains a large clearance from the top and inner wall. The purple triangles are from tiles in recessed areas of the inner wall and outer limiter side protection (Fig. 5). The dashed line shows the increase in bolometer radiation required to fix the energy deficit. Divertor tiles 3, 6 & 7 are off scale in this plot due to the large plasma load.

For this particular pulse the total energy found is 72MJ compared to an input of 98MJ. The breakdown is as follows: losses (E_{TClim} 3MJ, E_{TCdiv} 45MJ, E_{rad} 29MJ), inputs (E_{nbi} 77MJ, E_{oh} 24MJ). So we are missing a total of 26 MJ which if it is all due to an error in the radiated power alone would require that the radiated energy (and power) were underestimated by a factor of 1.9. In Fig. 9, the dashed line shows the impact of applying this factor uniformly. Where there is expected to be low plasma loading, the energy density from tile calorimetry is closest to the original bolometer analysis without any factors applied.

Areas not covered by tile calorimetry are the tiles just outside of the divertor. However, the total energy falling on Tiles 1 and 8 which cover the upper part of the inner and outer vertical targets (see Fig.1) is only 2.13MJ and 0.54MJ respectively. Therefore, even if we are missing the same amount again on the un-instrumented baffle tiles, the total is still small compared to the 26MJ energy deficit.

Similar analysis has been carried out on high radiation pulses but because the correction factor you would need on the radiation to explain the energy imbalance is smaller (~1.3) the result is less clear-cut than in low radiation cases. Further detail on this is given by Guillemaut [16].

5. Discussion

Despite significant progress in analysing the energy balance in JET we can only constrain the cause but not fully isolate it. We can however make the following statements:

Errors related to energy loss terms:

- A simple multiplier in the calibration of the bolometer derived power cannot explain the missing energy in a consistent way across the whole data set. Shots with high radiated power fraction would need a smaller correction factor than those with low radiation. The local energy density on tiles where there is minimal plasma contact, agrees well with numbers derived from the bolometers.

- If all the error is due to the analysis of the tile thermocouples then we need to increase our numbers by 70% when we consider 20% to be the maximum reasonable upper limit on the systematic error based on detailed simulation of the methods used. There will be some plasma losses outside of the divertor on the un-instrumented divertor baffles but all the evidence we have suggests that these are small and an allowance for this is already included in the error estimation.

Errors related to energy inputs:

- We have considered the possibility of systematic error in the neutral beam input energy which is the dominant input term. If this were the only issue we would need the beam power to be 20-35% lower than currently calculated. This must be compared to an extensive analysis of the neutral beam system which suggests a maximum systematic error of ±9.1%. This figure results from the following uncertainties: Voltage(<0.1%), ion current(<0.1%), neutralisation efficiency(±3%), transmission losses(±5.9%). Details of the methods used are described in [9]. Experiments have recently been carried out to see if there are any signs that the energy discrepancy depends on the neutral beam source position in the box, its voltage or its on-time but these have showed less than 3% variations in the energy balance with very similar missing fractions to the pulse discussed section 4.

- The ICRF power coupled to the plasma is given by the difference between the total power applied by the RF generators and the Ohmic losses in the transmission lines and antenna structures [10]. The former is inferred from forward and reflected voltage measurements taken with directional couplers installed in the transmission lines, and take into account the reflected power from the antenna due to eventual impedance mismatch between the generators and the antenna-plasma circuit. The reflected power is typically below 10% of the forward power when the system is properly matched. The Ohmic losses in the circuit are estimated from vacuum measurements and are proportional to the skin depth of the RF waves in the metallic structures and thus decrease with frequency. Typical values of the Ohmic losses of the JET A2 antenna strap at f=42MHz are around 0.5Ω. This value is significant compared to the common values of the antenna-plasma coupling resistance, ranging from ~0.8Ω in poor coupling conditions (e.g. H-mode or low SOL density) to ~2Ω (L-mode or optimized SOL density). The error-bars on the coupled ICRF power calculations are of the order of 10-15%, as a combination of (i) the uncertainties in the directional coupler measurements (misalignment, contribution of higher harmonics, etc.) and (ii) the difficulty of determining the exact Ohmic losses in the vacuum measurements due to the high Q of the circuit in these conditions. In addition, depending on antenna phasing, about 10% of input can be deposited on tiles specifically connected to the antenna [11] which are not part of the tile calorimetry system. Regressions do not point to a major issue with the ICRH input calculations and the imbalance exists in shots without ICRH heating so it can be eliminated as a primary cause of the imbalance.

- The formula used to calculate the Ohmic power in the EFIT equilibrium code comes from the poloidal magnetic energy balance equation [12]. The Ohmic heating is approximated by the dissipative term in this equation which is valid in the large aspect ratio, low beta limit. The other two terms are the time derivative of the poloidal magnetic energy and the Poynting term representing the energy flow across the boundary. The Poynting term is written as the product of the total toroidal current and the toroidal loop voltage on the plasma boundary. In EFIT, this voltage is calculated as the time derivative of the poloidal magnetic flux at the boundary. Evaluation of the statistical and systematic errors in these calculations is complex because it is linked to the errors in the magnetic equilibrium and such an analysis has not yet been carried out. Fortunately, this does not affect our main conclusions because we know that with high external energy input the Ohmic contribution is relatively small.

A compromise approach achieving energy balance is to assume we have systematic errors on all elements of the equation thus allowing us to meet somewhere in the middle as in case 4 of table 1. Alternatively, the linear approach could simply be wrong and that the errors actually scale in a more complex way.

If the missing energy is due to an unobserved loss inside the vessel then the area of deposition needs to be fairly large to avoid detection. Such a loss also must be roughly proportional to the total input energy or divertor energy rather than electromagnetic radiation. A possible contribution comes from the losses due to charge exchange around the entrance to the divertor on the inboard and outboard sides in the gap between the last instrumented divertor tile and first instrumented limiter tiles which would also not be seen by the bolometer cameras. These areas are obvious candidates for diagnostic improvements in the future.

6. Conclusions

To be fully confident that in current devices we have demonstrated integrated scenarios which respect the limits for PFCs in ITER and DEMO [13], accurate energy accounting is required since high radiated power fractions are needed. Even a few percent of input can potentially cause damage in ITER or DEMO if not deposited on a large area of PFCs. In JET, we typically can find ~ 75% of the calculated input energy. This suggests that the maximum achieved radiated power fraction (~75% of input) seen in JET with nitrogen seeding [14] tells us more about the accounting errors or unmeasured losses than it does about the residual power load on the divertor.

Although the source of the imbalance is still an open question, JET's energy balance studies have shown how scaling and other methods can be used to eliminate some of the possibilities and are pointing the way to new diagnostics for use in future studies which could fill gaps in our current data. Tokamaks are a complex system and it is clear that characterising and minimising the systematic errors in the energy balance is more important than having a set of numbers which appear to add up.

Acknowledgements

This work has been carried out within the framework of the EUROfusion Consortium and has received funding from the Euratom research and training programme 2014-2018 under grant agreement No 633053. The views and opinions expressed may not reflect those of the European Commission. This work was also part-funded by the RCUK Energy Programme under grant EP/I501045.

References

[1] G F Matthews et al., Phys. Scr. (2011) 014001

[2] G.F.Matthews et al., J. Nucl. Mater. 290-293 (2001) 668-672

[3] S.Devaux et al., J. Nucl. Mater. 438 (2013) S1208-1211

[4] C.Guillemaut et al., “Evidence for enhanced main chamber wall plasma loads in JET ITER-like Wall at high radiated fraction”, this conference.

[5] V.Riccardo et al., “Power footprint definition for JET divertor protection”, this conference

[6] P.Bunting, internal report ref: IVER_UM_1500_D014 issue 2, 12 Nov. 2015

[7] G.Arnoux et al., Nucl. Fusion 53 (2013) 073016 (12pp)

[8] D.E.Dombrowswski JET report, JET-IP (94)07, 1994

[9] H P L de Esch, A J Bickley ‘Where does the neutral beam power go?’ JET-DN-C(96) 137

[10] I. Monakhov et al., Nucl. Fusion, Vol.53, No.8, August 2013, p.083013

[11] P. Jacquet et al., J. Nucl. Mater. 438 (2013) S379–S383

[12] W.A.Houlberg, Nucl. Fusion, Vol.27. No.6 (1987) 1009

[13] R.P. Wenninger Nucl. Fusion 54 (2014) 114003 (8pp)

[14] M.Wischmaier, J. Nucl. Mater. 463 (2015) 22–29

[15] L.C. Ingesson, JET report JET-R(99)06

[16] C.Guillemaut et al. “Evidence for enhanced main chamber wall plasma loads in JET ITER-like Wall at high radiated fraction” to be published in the proceedings of the 22nd International Conference on Plasma Surface Interactions, Rome (2016)